3D simulation of rotating spoke in a wall-less Hall thruster

IEPC-2019-437

Presented at the 36th International Electric Propulsion Conference
University of Vienna • Vienna, Austria
September 15-20, 2019

K. Matyash[1], R. Schneider[2],
Greifswald University, Greifswald, D-17487, Germany

Abstract: The low-frequency rotating plasma instability (spoke) in the ISCT200WL wall-less Hall thruster was simulated with a 3-dimensional PIC MCC code. In the simulations an $m = 1$ spoke rotating with a velocity of 6.5 km/s in the ExB direction was observed. The rotating electron density structure in the spoke is accompanied by a strongly depleted region of the neutral gas. The magnetic field reversal in the simulation did not cause the change of the spoke rotation direction, the spoke continued to move toward the higher neutral density, opposite to the ExB direction, which excludes the electron drift-type instabilities from the possible origins of the spoke rotation. When a void with an azimuthal length of 5-7 mm was introduced in the neutral density profile by suppressing the gas feeding at the small sector of the ring anode, the spoke was not able to transit through the emerged void. These results clearly show that the spoke rotation is determined by the propagation of the ionization front, rather than by some kind of electrostatic instability. The spoke is an ionization driven instability, similar to the axial breathing mode. Coexistence of the m=1 spoke and the axial breathing oscillations was observed in the simulations. The frequency of the spoke rotation was twice higher than the breathing mode frequency. It was found that for strongly coupled breathing mode and the spoke oscillations their frequencies should be related as $f_{BM} = (n+1/2)f_{Sp}$.

Nomenclature

B	=	magnetic field
E	=	electric field
f_{Sp}	=	spoke rotation frequency
f_{BM}	=	breathing mode frequency
c_s	=	ion acoustic speed
$\dot{m}$	=	mass flow rate
n_e	=	electron density
t	=	time
T_e	=	electron temperature
T_n	=	neutral temperature
I	=	electric current
U_a	=	anode voltage
Δx	=	cell size
X, Y, Z	=	coordinates
Δt	=	time step
ϕ	=	electric potential
φ	=	oscillation phase

[1] Head of HPC group, Greifswald University, knm@ipp.mpg.de
[2] Professor, Greifswald University, Head of Computer Center, schneider@uni-greifswald.de

I. Introduction

The low-frequency rotating plasma instability, often called the "rotating spoke", is a phenomenon frequently observed in various *E*x*B* cross-field discharges like Hall thrusters, magnetrons and plasma columns[1]. In Hall thrusters, despite decades of investigation, the origin, dynamics and nature of the spoke are still not fully understood. The earliest spoke study, carried out by Janes and Lowder[2], identified an azimuthal structure moving at tens of kilometers per second, whose presence was later attributed to the ionization type instability[3]. Our recent Particle-in-Cell with Monte Carlo collisions (PIC MCC) simulations of the cylindrical Hall thruster (CHT)[4] have also pointed out the ionization nature of the spoke instability. However, this hypothesis still needs to be validated both theoretically and experimentally.

In a Hall thruster, the spoke instability is of importance because it has been shown to be present under any operating conditions, with the mode number varying according to the thruster size and operating conditions[5]. The rotating spoke is of particular interest because it can conduct current, thereby participating in anomalous electron transport across the magnetic field[5-7]. Measurements performed in a CHT thruster have demonstrated that a large fraction of electron current towards the anode flows through the spoke[6,7]. Probe measurements of the time-evolution of the azimuthal electric field also revealed that the electric field generated by the spoke is responsible for axial electron current.

In this work we apply the 3D PIC MCC code STOIC[4,8-10] to investigate the properties of low-frequency rotating plasma instabilities in the discharge of the low-power ISCT200 Hall thruster[11,12] operating in the wall-less configuration[13-16]. In a wall-less configuration the anode is moved towards the channel exit, so that the ionization and the acceleration regions are located outside the thruster cavity. A photograph of the ISCT200 Hall thruster in WL configuration with its gridded anode at the channel exit is displayed in Figure 1. The same figure shows the ISCT200-WL thruster firing with Xe at 1 mg/s and 200 V discharge voltage. As can be seen from this image, the plasma discharge is detached from the anode - the signature of an efficient confinement. A wall-less ion source provides an ideal platform for the study of electron transport in cross-field discharge configurations as the discharge is easily accessible for diagnostics. The main objective of this work was to characterize the dynamics of rotating plasma structures in the *ExB* discharge of an ISCT200-WL thruster and to provide insight into the physics of the rotating spoke instability by means of self-consistent PIC simulations.

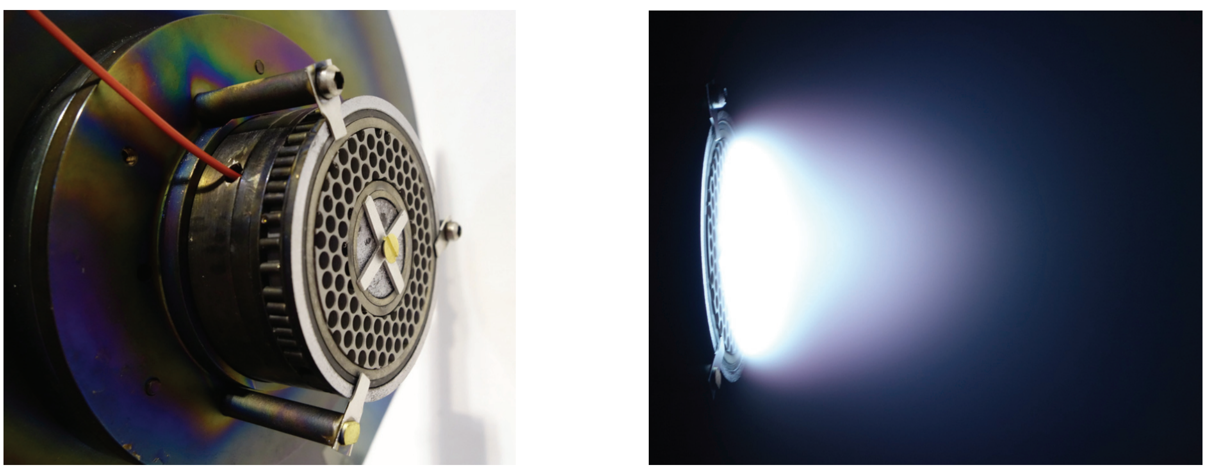

Figure 1. The ISCT200 Hall thruster in WL configuration with a gridded anode at the channel exit plane (left) and the ISCT200-WL thruster firing with Xe in the NExET test bench.

II. The model

In this work, the self-consistent 3D-3V Particle-in-Cell simulation code STOIC (electroSTatic Optimized particle In Cell)[4,8-10] has been applied to simulate the rotating spoke instability in the ISCT200 thruster operating in the wall-less configuration[14-16]. The simulation includes electrons, Xe^+ ions and neutral Xenon atoms. All relevant collisional processes are included in the model via Monte Carlo collision algorithms: Coulomb collisions between charged particles; electron-neutral elastic, ionization and excitation collisions; ion-neutral momentum transfer and charge exchange collisions and neutral-neutral elastic collisions. The dynamics of the background neutral gas is selfconsistently resolved with direct simulation Monte Carlo (DSMC). The model is fully 3D - 3 spatial and 3 velocity components are resolved. It utilizes an equidistant Cartesian grid which explicitly assures momentum conservation and zero self forces.

The computational domain represents a cuboid with length $Z_{max} = 50$ mm and sides $X_{max} = Y_{max} = 70$ mm. The Z axis is directed along the thruster symmetry axis. The sketch of the computational domain together with magnetic field topology and particle sources is shown in Fig. 2. The plane $Z = 0$ corresponds to the channel exit, where the anode (red) is placed. The ring anode is mapped with the Cartesian mesh. All boundaries of the computational domain are assumed to be metallic. All metal elements in the simulation, except for the anode are at ground potential (blue). At the anode, a voltage of $U_a = 225$ V is applied. The neutrals are injected into the system uniformly through the anode with the mass flow rate $\dot{m} = 0.8 - 1$ mg/s and $T_n = 1100$ K. Electrons with a Maxwellian distribution and a temperature $T_e = 2$ eV are introduced into the system in the source region $42\,\text{mm} < Z < 46\,\text{mm}$, $26\,\text{mm} < R < 30\,\text{mm}$ with uniform density and the constant current $I_c = 0.25$ A, simulating the thruster cathode. All surfaces in the simulation are assumed to be absorbing for electrons and ions. No secondary electron emission is included in the simulation. The neutrals are lost on all surfaces, except for the anode plane, where they are re-launched with a Maxwellian distribution with the temperature $T_n = 1100$ K.

To reduce the computational time the size of the system is scaled down by a factor of 10. In order to preserve the ratio of the particles' mean free paths and the gyroradii to the system length, the collision cross-sections and the magnetic field are increased by the same factor of 10.

An equidistant computational grid 70x70x50 was used in the simulation. The total number of computational particles in the simulation was about $1.6 \cdot 10^8$. The cell size $\Delta x = \Delta y = \Delta z = 0.1$ mm in the simulation was chosen to ensure that it is smaller than the smallest Debye length in the system. The time step was set to $\Delta t = 5.6 \cdot 10^{-12}$ s in order to resolve the electron plasma and cyclotron frequencies. The simulations were carried on a 16-processor Intel Xeon workstation, with longest run duration of about 50 days. About $1.8 \cdot 10^7$ time steps were performed, corresponding to a simulated time of 100 μs.

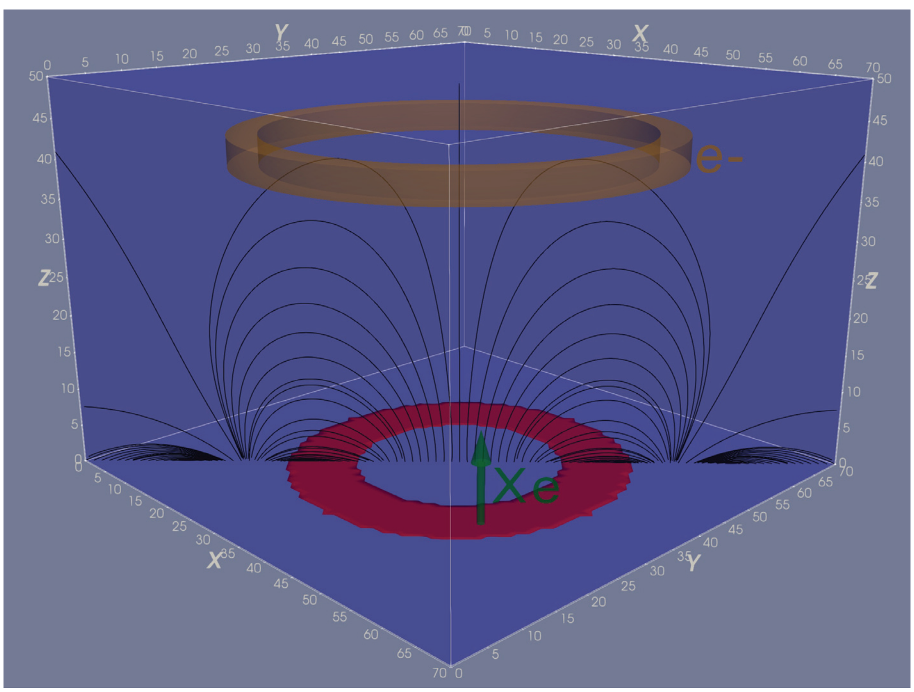

Figure 2. Computational domain with magnetic field topology and particle sources.

III. Simulation results

In the simulation, after a start up transient of about 5 μs, the rotating spoke instability develops in the ionization region close to the anode. In Figure 3 the evolution of electron density *XY* cross-section 3 mm above the anode during the spoke cycle is shown. The $m = 1$ mode spoke is rotating in the *E*x*B* direction (clockwise) with the average velocity 6.5 km/s, which corresponds to the rotation frequency of 57 kHz in the real (unscaled) geometry. The spoke rotation velocity in the simulation is about a factor of 3 higher than observed in the experiment[15,16]. Such discrepancy with the experimental results may be caused by the proximity of the domain boundaries to the discharge plasma in the simulations and by the applied geometrical scaling. After its development the spoke is present until the end of the simulated time of 100 μs and demonstrates a very regular pattern. The spoke rotation period fluctuation level throughout the simulation is below 5%. In Figure 4 the evolution of the plasma density along the spoke median line (the circle of radius 18 mm, 3 mm above the anode) during 10 spoke rotation cycles is shown. In total 55 full spoke cycles occur during the simulated time.

In the previous simulations in addition to the m=1 spoke rotating in the *E*x*B* direction, we also observed m=1 and m=2 spokes rotating in the counter-*E*x*B* direction[9]. The spoke rotation direction and the mode number were dependent on the applied anode voltage and neutral gas flow from the anode source.

In Figure 5 the evolution of the electron and neutral density, ionization rate and plasma potential along the spoke median line during the spoke cycle is presented. The spoke moves from right to left, which corresponds to counter-clockwise rotation. Higher plasma density in the spoke and associated space charge result in the local elevation of the plasma potential, which reaches up to 260 V, higher than the anode voltage $U_a = 225$ V. The rotating electron density structure is accompanied by the strongly (up to 75%) depleted region of the neutral gas, which clearly shows that the spoke instability is of the ionization type. As the largest part of the neutrals are locally consumed by electron-impact ionization, the ionization front moves further toward the region with higher neutral density. The void in the neutral gas, which is left behind the ionization front, then is gradually refilled by the gas flux from the anode source, such that the neutral density is restored to the previous level before the ionization front makes the full turn, so that the cycle can recur. This process looks rather similar to the breathing mode oscillations[17, 18], where the neutral gas front moves back and forth in the axial direction due to predator-prey-like dynamics between the electrons and the neutrals. But in contrast to the breathing mode, the spoke instability does not manifest itself in the discharge current, as the plasma density averaged over the discharge transverse cross-section stays constant as the spoke rotates.

Another important feature visible in Fig. 5 is that in addition to the macroscopic spoke structure, there are short-scale (2-4 mm) oscillations present in the electron density, plasma potential and the ionization rate. These short-scale oscillations have the frequencies in the in 4-10 MHz range[9] and likely are responsible for the electron transport through the spoke core.

In fact, recent measurements by coherent Thomson scattering on a wall-less version of a 1.5 kW thruster indeed show the coexistence of oscillations in the same high-frequency range (associated with the electron cyclotron drift instability[19]) with spokes. These observations will be discussed in detail in future work. The small-scale turbulence inside the rotating spoke was also observed in the CHT thruster experiment[20].

In Figure 6 the axial and azimuthal electric field along the spoke median line are plotted. In the spoke core ($61\,\mathrm{mm} < X < 103\,\mathrm{mm}$) short-scale, high-frequency (HF) oscillations with the electric field amplitude about 100 V/cm (both axial and azimuthal) are present. The mean electric field in the spoke core is much lower, below 5 V/cm (both axial and azimuthal), thus the regular azimuthal *E*x*B* drift of electrons inside the spoke bulk is impossible and the electron dynamics is determined by the short-scale HF oscillations. The axial electric field, averaged over the spoke cycle, is about 60 V/cm, which corresponds to an *E*x*B* drift velocity of 188 km/s. This is about 30 times higher than the spoke velocity of 6.5 km/s.

The regular azimuthal *E*x*B* drift is possible only at the spoke front ($3\,\mathrm{mm} < X < 61\,\mathrm{mm}$) and the spoke rear ($103\,\mathrm{mm} < X < 113\,\mathrm{mm} \ \cup \ 0\,\mathrm{mm} < X < 3\,\mathrm{mm}$) where the axial electric field does not change its sign. In the spoke front the axial electric field grows from ~50 V/cm to ~200 V/cm so that the azimuthal electron *E*x*B* drift is accelerated by a factor 4 – from 157 km/s to 630 km/s. The azimuthal electric field for most of the spoke front ($12\,\mathrm{mm} < X < 61\,\mathrm{mm}$) is directed counter-clock-wise with the average value about 20 V/cm, which means that there exists an axial electron *E*x*B* drift directed toward the anode with average velocity of about 63 km/s, which contributes to the anode current. These two effects: rapid acceleration of the azimuthal electron *E*x*B* drift and the loss of the electrons at the anode, lead to a decrease of the electron density at the spoke front, preventing the spoke from spreading forward. On the opposite side of the spoke, the ionization rate drop associated with the neutral density decrease prevents the spoke from spreading backward, so that the spoke propagates as a coherent structure.

In order to validate the hypothesis of the ionization nature of the spoke instability we instantly (during one PIC time step $\Delta t = 5.6 \cdot 10^{-12}$ s) reversed the direction of the magnetic field in the simulation. Such a rapid change of the magnetic field would be impossible in the real experiment due to the finite inductance of the magnetic coils, so this is a purely computational experiment. In Figure 7 the evolution of the plasma and the neutral density along the spoke median line during 17.34 μs is shown. The magnetic field reversal takes place exactly in the middle of the presented time domain, at 8.67 μs. As one can see after the B-field reversal the spoke does not change its rotation direction, continuing to move toward the higher neutral density region, in counter- *E*x*B* direction, although its velocity decreases from 6.5 km/s to 3.9 km/s. This result excludes the electron drift type instabilities as a possible origin of the spoke rotation.

Another interesting validation case is the propagation of the spoke across the neutral density void. Following the idea from the Ref. 21 we introduced the neutral density void in the simulation shutting down the neutral gas flux at the small sector of the anode source. In Fig. 8 the evolution of the plasma and the neutral density along the spoke median line 2 mm above the anode during 17.34 μs is shown. The gas flux was shut down at the sector of 16^o at the 8.67 μs, after the largest part of the spoke structure has passed over it. The spatiotemporal position of the closed part of the gas inlet is marked in Fig. 8. In Fig. 8(right) one can see the neutral density void developed 2 mm above the anode. The azimuthal dimension of the void is about 5 mm, which is much shorter than the spoke length of ~ 35 mm. So, if the spoke would propagate due to electron motion in some sort of electrostatic instability, such short perturbation of the neutral density would not affect its motion. However this is not the case, as one can see in the spatiotemporal diagram of the plasma density in Fig.8(left). The spoke does not actually transit through the neutral gas void. Instead, the spoke stops, when it reaches the edge of the void, and the new spoke structure develops on the opposite side of the void in the region where the neutral density has its maximum, while the original one fades out as the neutrals are consumed. The plasma density inside the neutral void is always negligible compared to the plasma density in the spoke. This behavior is even more apparent in the case of larger voids. In Fig. 9 the spatiotemporal profiles of the neutral and the plasma density for the void of ~ 7 mm (the anode sector of 22.5^o was shut down) are presented. As one can see in Fig. 9(left) the new spoke can develop ~20 mm from the void edge (t = 15 μs), where the neural density has its maximum. Thus we can conclude that in the simulations the spoke rotation is due to propagation of the ionization front rather than because of some kind of electrostatic instability. The spoke is the ionization driven instability, similar to the axial breathing mode.

In the simulations a regime was found where the m=1 spoke rotating in the *ExB* direction coexists with the axial breathing mode. Corresponding plots for spatiotemporal profile of the plasma and neutral density along the spoke median line 2 mm above the anode are presented in Fig. 10. The frequency of the breathing oscillations measured in the anode current was $f_{BM} = 18.91$ kHz, the anode current modulation level was about 65%. The spoke rotation frequency measured in the electron density 2 mm above the anode was $f_{Sp} = 38.6$ kHz. This is almost exactly two times higher than the breathing oscillations frequency ($f_{Sp}/f_{BM} = 2.04$), which can be also seen in Fig.10. In Figure 11 the evolution of the electron and neutral density at the spoke radius $R_{Sp} = 18$ mm during a breathing oscillation cycle is presented. In Figure 11a one can see that when the spoke reaches the maximum plasma density around $S = 55 - 80$ mm, it leaves the deepest hole in the neutral background at that position, where it consumes the maximal amount of neutrals by ionization. So, when the spoke returns to the same azimuthal position after one rotation cycle, it experiences the minimum neutral density. This leads to the drop of the plasma density to its minimum due to the reduction of the ionization rate (Fig. 11b). This time the spoke creates the shallowest hole in the neutral density. After the next spoke rotation cycle, the spoke gets the neutral density maximum, which leads to the growth of the plasma density to its maximum again (Fig. 11c). Thus, due to such predator-prey dynamics, in two cycles of the spoke rotation the axial breathing mode is completing one full oscillation cycle.

Generalizing this picture we can say that if the azimuthal spoke and the axial breathing mode coexist and are strongly coupled, due to the fact that the spoke gives the negative feedback to the breathing mode through the neutral background and the feedback time equals one spoke rotation cycle, in order to be in the resonance the axial breathing oscillation after one spoke cycle should change its phase by 180^o (i.e. one spoke rotation cycle should correspond to the odd number of the breathing mode half-cycles). This leads to the relation between the spoke and breathing mode frequencies:

$$f_{BM} = \left(n + \tfrac{1}{2}\right) f_{Sp}\text{, where } n \in \mathbb{N} \tag{1}$$

From Eq. 1 it follows that the only case when the spoke frequency is higher than the breathing mode frequency is $f_{Sp} = 2f_{BM}$. This is the case observed in the simulation.

There is too little experimental data available for the simultaneous measurements of the spoke and breathing oscillations frequencies to validate the Eq. 1. In the recent work of Romadanov et. al.[22] the spoke with frequency 8.6 kHz and the breathing oscillation 13.8 kHz were measured simultaneously, which is within 10% agrees with the Eq. 1 for $n = 1$. Moreover the damping of the spoke by the externally exited breathing oscillations observed in Ref. 22 may be caused by desynchronization of the rotating spoke with the axial breathing mode.

Strictly speaking the separation of the oscillations into the spoke and the breathing mode in the discussion above is nominal - in the simulation we observe single low frequency ionization instability, which manifests itself both azimuthally and axially.

IV. Conclusion

The rotating spoke instability in the ISCT200WL wall-less Hall thruster was simulated with a 3-dimensional PIC MCC code. In the simulations an m = 1 spoke rotating with a velocity of 6.5 km/s in the ExB direction was observed.

Strong high-frequency electric field oscillations, with a frequency in the range of 4-10 MHz, a length scale of about 3 mm and amplitudes of the order of 100 V/cm were observed inside the spoke core. These electric field oscillations have characteristics very similar to the electron cyclotron drift instability (frequency, length scale) observed experimentally in recent years in both thrusters and planar magnetrons[23,24], and are further evidence for its likely role in electron transport.

The rotating electron density structure in the spoke is accompanied by a strongly depleted (up to 75%) region of the neutral gas. The instant magnetic field reversal in the simulation did not cause the change of the spoke rotation direction, the spoke continued to move toward the higher neutral density, opposite to the ExB direction, which excludes the electron drift-type instabilities from the possible cause of the spoke rotation. When the void of the azimuthal length of 5-7 mm was introduced in the neutral density profile by suppressing the gas feeding at the small sector of the ring anode, the spoke was not able to transit through the emerged void. These results clearly show that the spoke rotation is determined by the propagation of the ionization front, rather than by some kind of electrostatic instability. The spoke is the ionization driven instability, similar to the axial breathing mode.

Coexistence of the m=1 spoke and the axial breathing oscillations was observed in the simulations. The frequency of the spoke rotation was twice higher than the breathing mode frequency. It was suggested that in general case of coupled breathing and spoke oscillation one spoke rotation cycle should correspond to the odd number of the breathing mode half-cycles (Eq.1).

Acknowledgments

The Authors would like to thank Dr. Sedina Tsicata, Dr. Stéphane Mazouffre and Lou Grimaud for helpful discussions.

References

[1]J. P. Boeuf, Rotating structures in low temperature magnetized plasmas - insight from particle simulations, Frontiers in Physics, Vol 2, Art. 74, 2014, pp. 1-17.

[2]G. S. Janes and R. S. Lowder, "Anomalous electron diffusion and ion acceleration in a low-density plasma," Phys. Fluids, Vol. 9, No.6, 1966, pp. 1115–1123.

[3]Y. V. Esipchuk, A. I. Morozov, G. N. Tilinin, and A. V.Trofimov, "Plasma oscillations in closed-drift accelerators with an extended acceleration zone," Sov. Phys.-Tech. Phys., vol. 43, 1973, pp. 1466–1473.

[4]K. Matyash , R. Schneider , O. Kalentev , Y. Raitses and N. J. Fisch, "Numerical investigations of a cylindrical Hall thruster," 32nd International Electric Propulsion Conference, 2011, IEPC-2011-070.

[5]M. S. McDonald and A. D. Gallimore, "Parametric investigation of the rotating spoke instability in Hall thrusters," 32nd International Electric Propulsion Conference, 2011, IEPC-2011-242.

[6]J. B. Parker, Y. Raitses, and N. J. Fisch, "Transition in electron transport in a cylindrical Hall thruster," Appl. Phys. Lett., vol. 97, No. 9, 2010, p. 091501.

[7]C. L. Ellison, Y. Raitses and N. J. Fisch, "Cross-field electron transport induced by a rotating spoke in a cylindrical Hall thruster," Phys. Plasmas, 19, 2012, 013503.

[8]K. Matyash, R. Schneider, S. Mazouffre, Y. Raitses, and A. Diallo, "3D simulation of rotating spoke in a Hall thruster," 33rd International Electric Propulsion Conference, 2013, IEPC-2013-307.

[9]K. Matyash, R. Schneider, S. Mazouffre, L. Grimaud, and S. Tsikata, "Investigation of rotating spoke instabilities in a wall-less Hall thruster. Part II: Simulation," 35th International Electric Propulsion Conference, 2017, IEPC-2017-403.

[10]K. Matyash, R. Schneider, S. Mazouffre, L. Grimaud, and S. Tsikata, "Rotating spoke instabilities in a wall-less Hall thruster: simulations", Plasma Sources Sci. Technol., 28, 2019, 044002.

[11]S. Mazouffre, G. Bourgeois, K. Dannenmayer, and A. Lejeune, "Ionization and acceleration processes in a small, variable channel width, permanent-magnet Hall thruster," J. Phys. D: Appl. Phys., vol. 45, No. 18, 2012, p.185203.

[12]Lejeune, G. Bourgeois, and S. Mazouffre, "Kr II and Xe II axial velocity distribution functions in a cross-field ion source," Phys. Plasmas, Vol. 19, No. 7, 2012, p. 073501.

[13]S. Mazouffre, S. Tsikata, and J. Vaudolon, "Development and experimental characterization of a wall-less Hall thruster," J. Appl. Phys., Vol. 116, No.24, 2014, p. 243302.

[14]J. Vaudolon, S. Mazouffre, C. Henaux, D. Harribey, and A. Rossi. "Optimization of a wall-less Hall thruster," Appl. Phys. Letter, Vol. 107, No. 17, 2015, p. 174103.

[15]S. Mazouffre, L. Grimaud, S. Tsikata, K. Matyash and R. Schneider, "Investigation of rotating spoke instabilities in a wall-less Hall thruster. Part I: Experiments," 35th International Electric Propulsion Conference, 2017, IEPC-2017-248.

[16]S. Mazouffre, L. Grimaud, S. Tsikata, K. Matyash, and R. Schneider, "Rotating spoke instabilities in a wall-less Hall thruster: Experiments," Plasma Sources Sci. Technol., 28, 2019, 054002.

[17]J.P. Boeuf and L. Garrigues, "Low frequency oscillations in a stationary plasma thruster," J. App. Phys. 84, 1998, 3541.

[18]S. Barral and E. Ahedo, "Low-frequency model of breathing oscillations in Hall discharges," Phys. Rev. E 79, 2009, 046401.

[19]D. W. Forslund, R. L. Morse, and C. W. Nielson, "Electron Cyclotron Drift Instability," Phys. Rev. Lett., 25, 1970, 1266.

[20]C. L. Ellison, Y. Raitses, and N. J. Fisch, "Cross-field electron transport induced by a rotating spoke in a cylindrical Hall thruster," Phys. Plasmas 19, 2012, 013503.

[21]J Bak, R. Kawashima, K. Komurasaki, and H. Koizumi, "Plasma formation and cross-field electron transport induced by azimuthal neutral inhomogeneity in an anode layer Hall thruster," Phys. Plasmas, 26, 2019, 073505.

[22]I. Romadanov, Y. Raitses, and A. Smolyakov, "Control of coherent structures via external drive of the breathing mode," Plasma Phys. Rep., 45, 2019, 134.

[23]S. Tsikata, N. Lemoine, V. Pisarev and D. Gresillon, "Dispersion relations of electron density fluctuations in a Hall thruster plasma, observed by collective light scattering," Phys. Plasmas, 16, 2009, 033506.

[24]S. Tsikata and T. Minea, "Modulated Electron Cyclotron Drift Instability in a High-Power Pulsed Magnetron Discharge," Phys. Rev. Lett., 114, 2015, 185001.

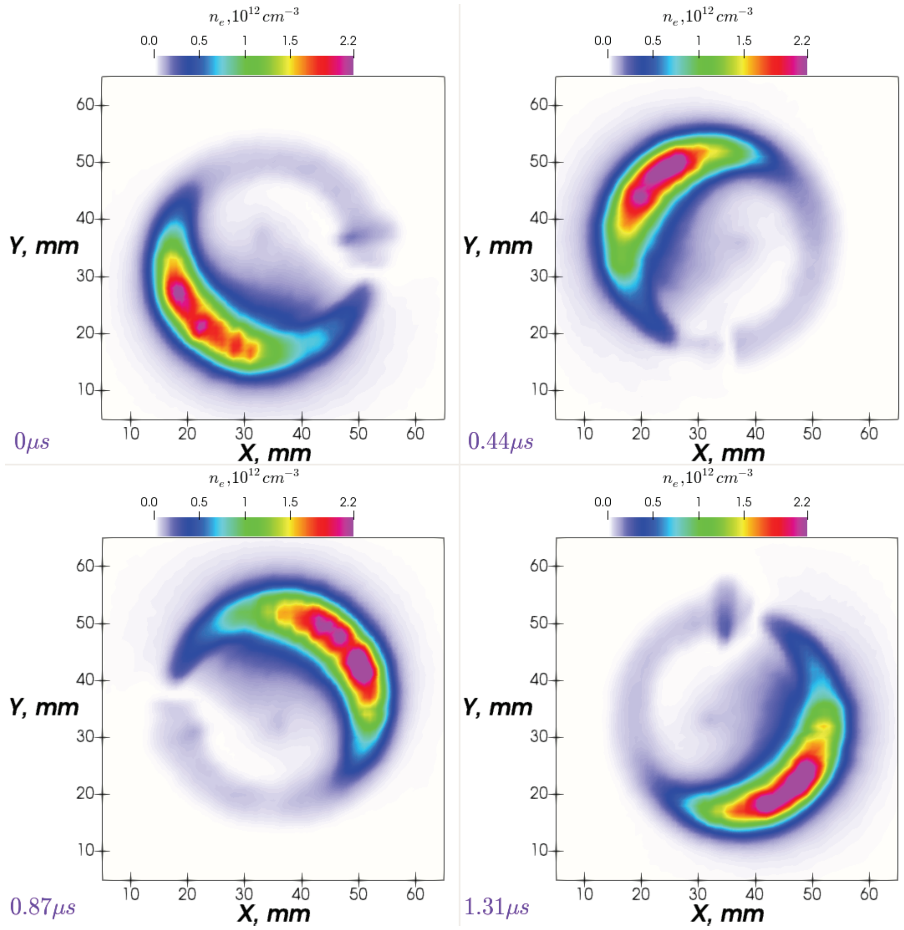

Figure 3. Evolution of the plasma density 3 mm above the anode during the spoke cycle. The spoke m = 1 rotates in the *E*x*B* direction with a velocity of 6.5 km/s.

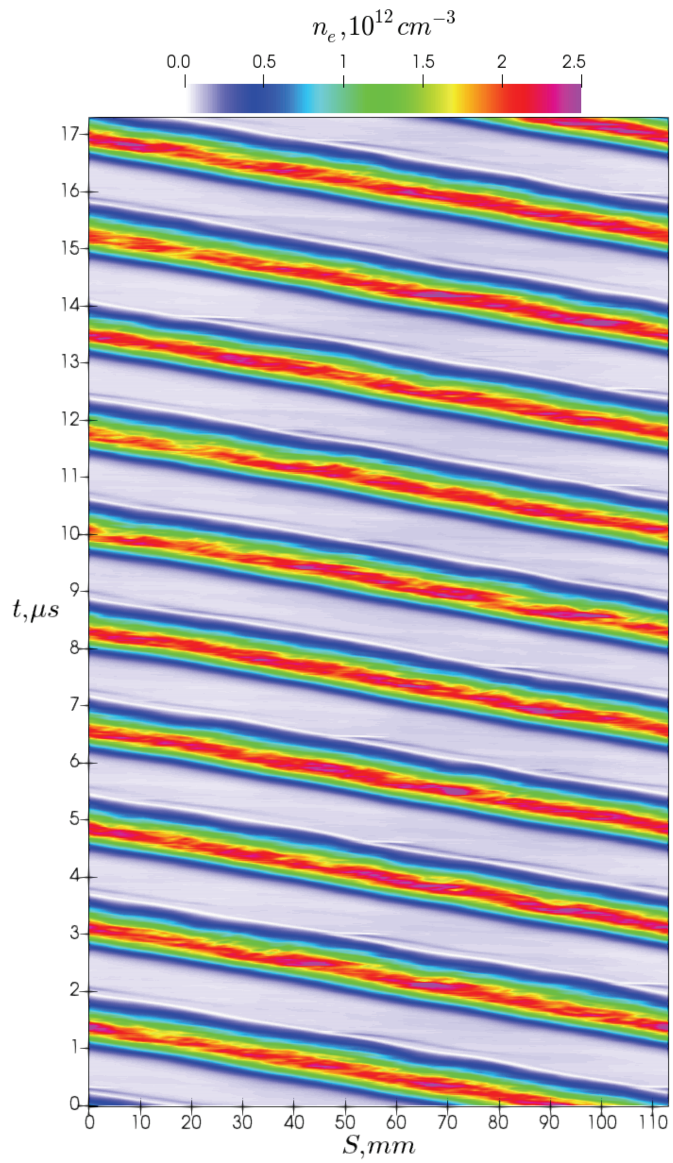

Figure 4. Evolution of the plasma density along the spoke median line (circle of radius 18 mm, 3 mm above the anode) during 10 spoke cycles. The distance S is measured counter-clockwise. The spoke m = 1 rotates in the ExB direction with a velocity of 6.5 km/s.

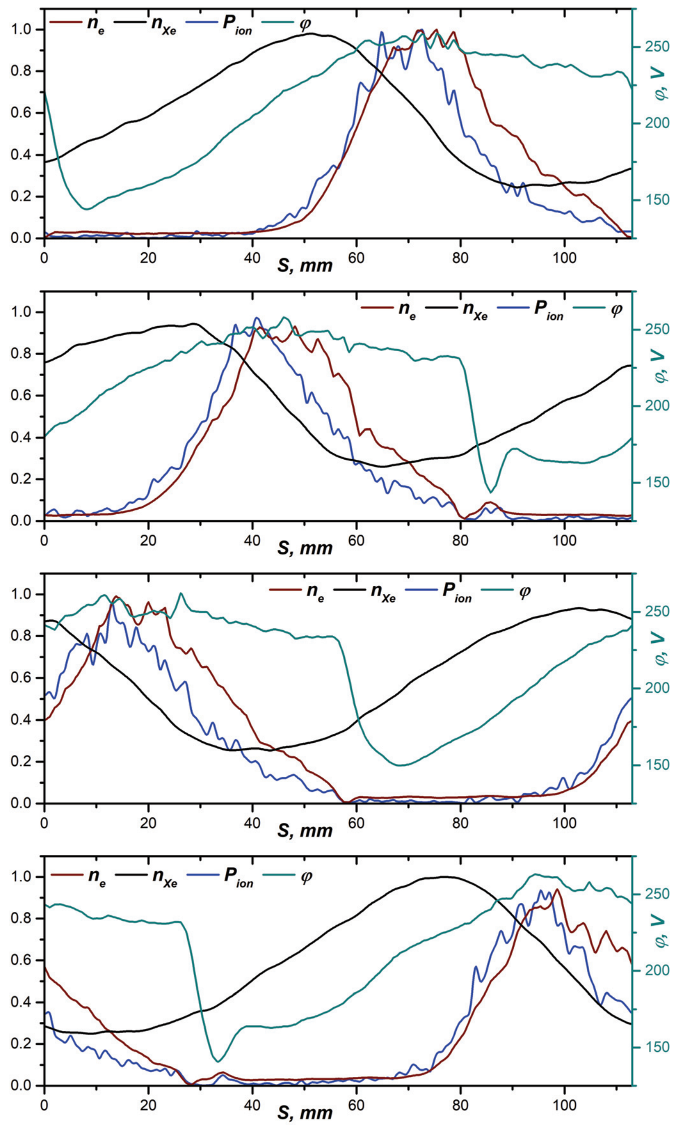

Figure 5. Electron and neutral density, ionization rate and plasma potential along the spoke median line (circle of radius 18 mm, 3 mm above the anode) during the spoke cycle. From top to bottom: t=0µs, t=0.44µs, t=0.87µs, t=1.31µs. The distance S is measured counter-clockwise. n_e is normalized by $2.3\cdot10^{12}$ cm^{-3}, n_{Xe} – by $1.2\cdot10^{13}$ cm^{-3}, P_{ion} – by $2.7\cdot10^{18}$ cm^{-3}s^{-1}.

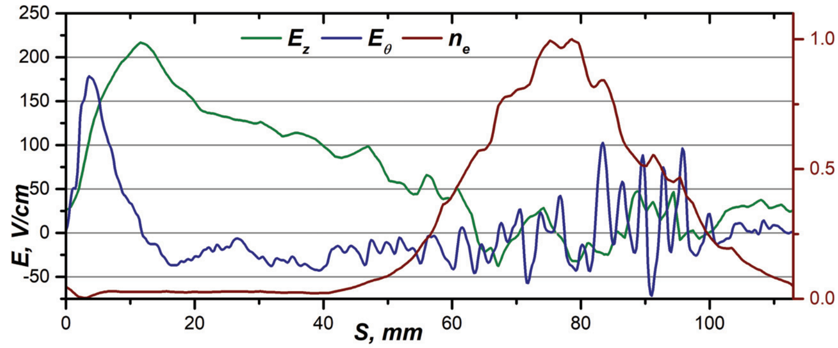

Figure 6. Axial and azimuthal electric field along the spoke median line. Normalized electron density is plotted for the reference.

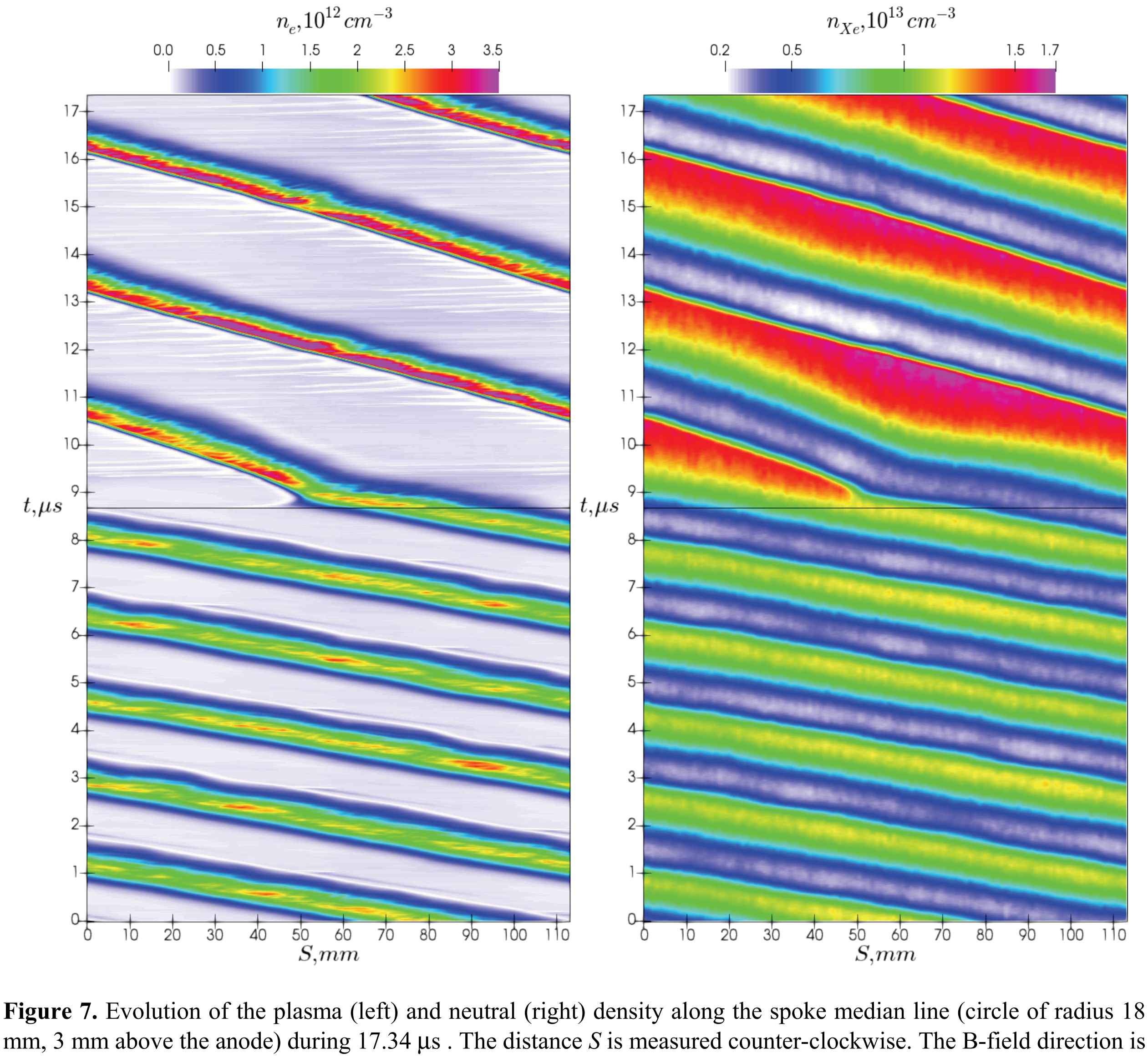

Figure 7. Evolution of the plasma (left) and neutral (right) density along the spoke median line (circle of radius 18 mm, 3 mm above the anode) during 17.34 µs . The distance *S* is measured counter-clockwise. The B-field direction is reversed at *t*= 8.67 µs (marked with horizontal line).

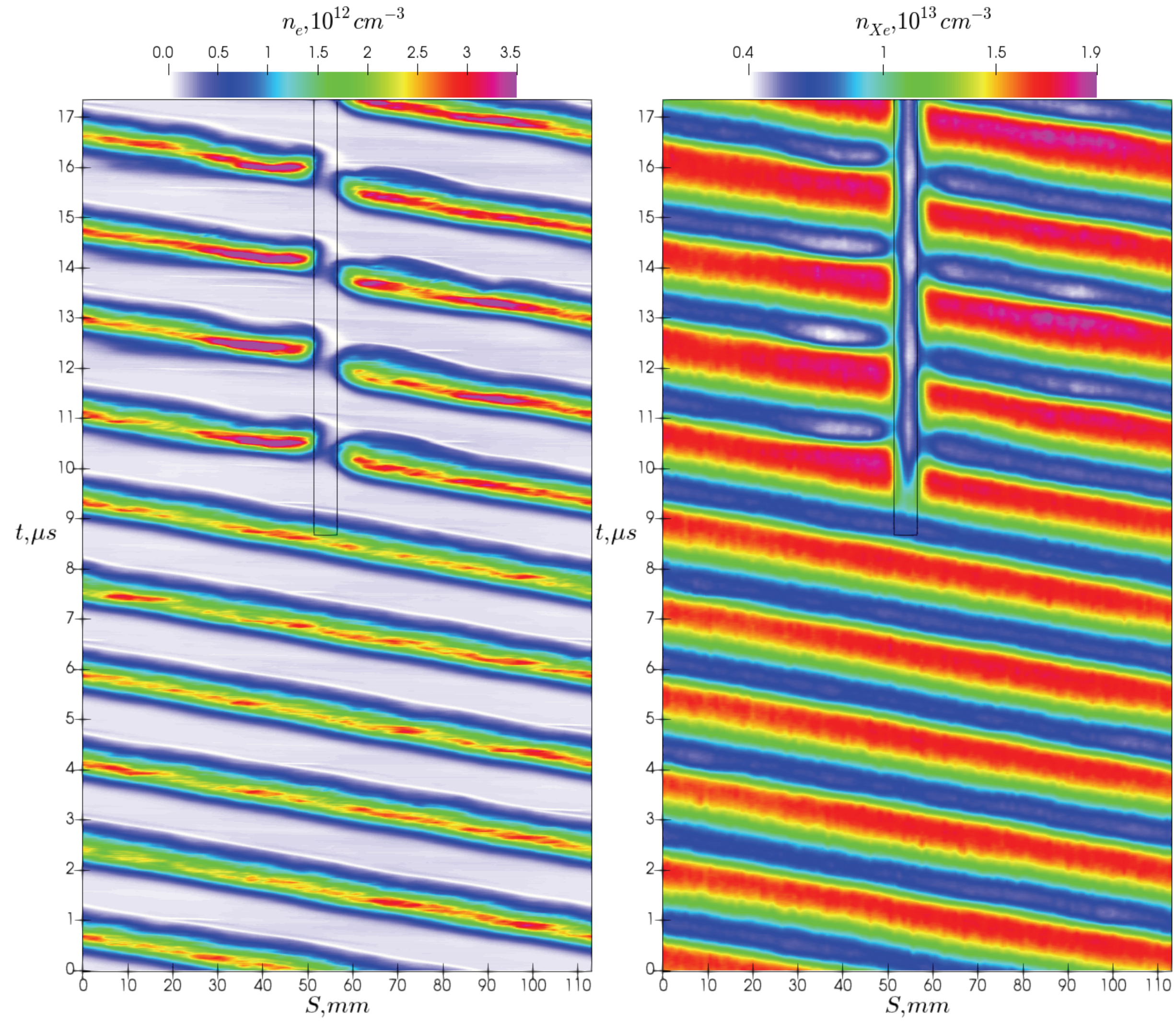

Figure 8. Evolution of the plasma (left) and neutral (right) density along the spoke median line (circle of radius 18 mm, 2 mm above the anode) during 17.34 µs. The distance *S* is measured counter-clockwise. The 16° sector of ring the gas inlet was shut down at *t*= 8.67 µs. The spatiotemporal position of the closed part of the gas inlet is marked with black line.

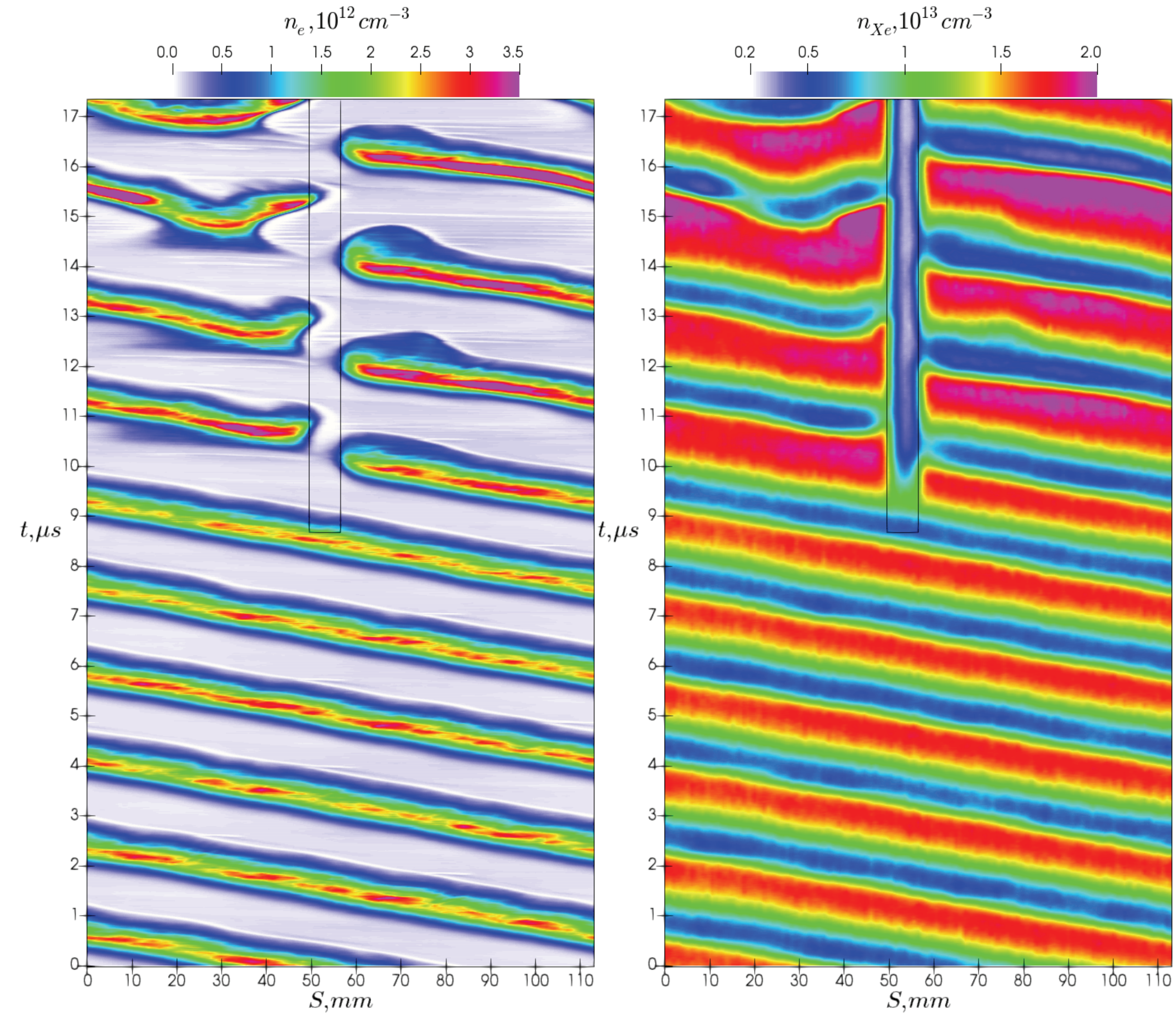

Figure 9. Evolution of the plasma (left) and neutral (right) density along the spoke median line (circle of radius 18 mm, 2 mm above the anode) during 17.34 µs. The distance *S* is measured counter-clockwise. The 22.5° sector of ring the gas inlet was shut down at *t*= 8.67 µs. The spatiotemporal position of the closed part of the gas inlet is marked with black line.

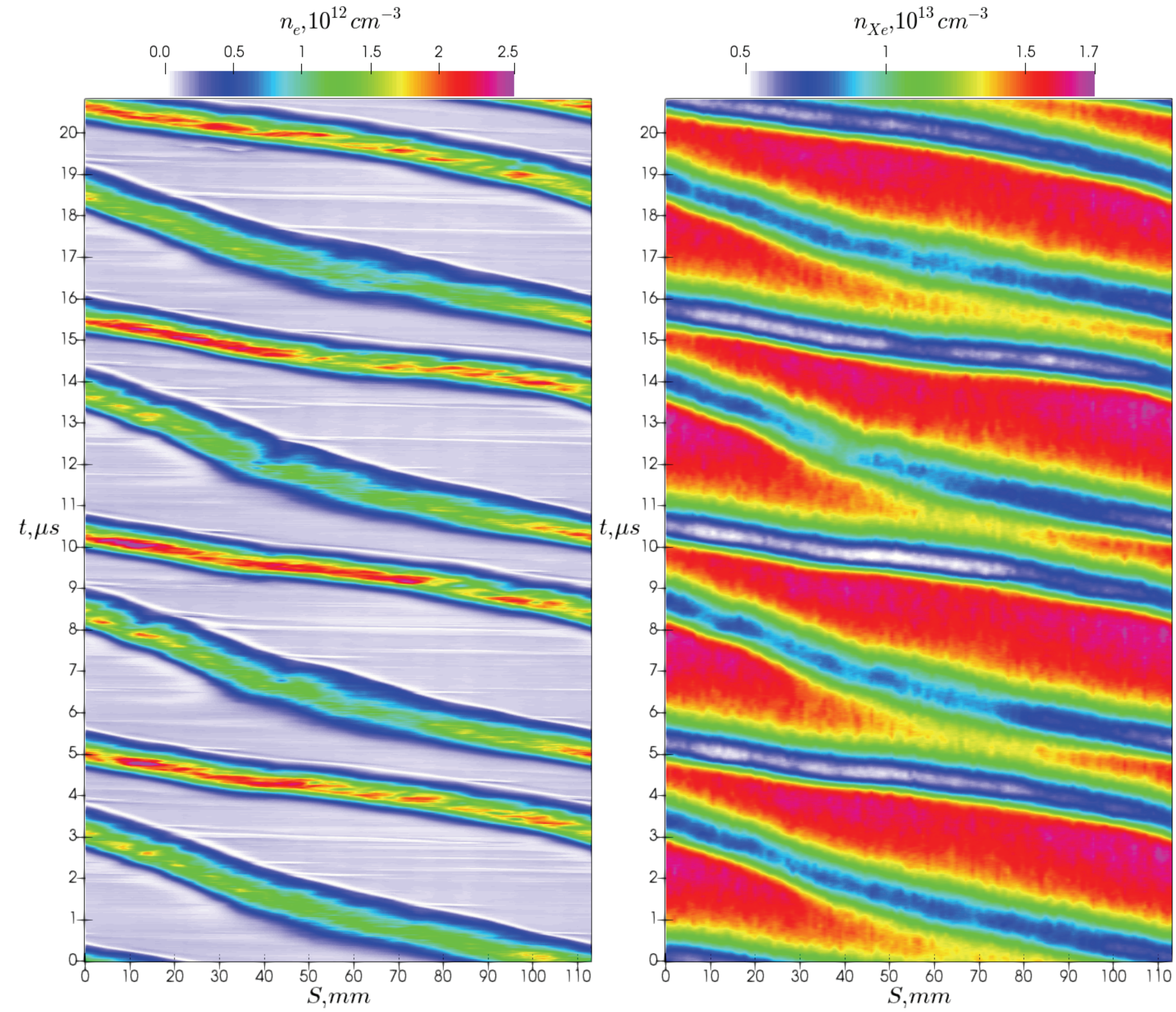

Figure 10. Evolution of the plasma (left) and neutral (right) density along the spoke median line (circle of radius 18 mm, 2 mm above the anode) during 8 spoke cycles. The distance *S* is measured counter-clockwise.

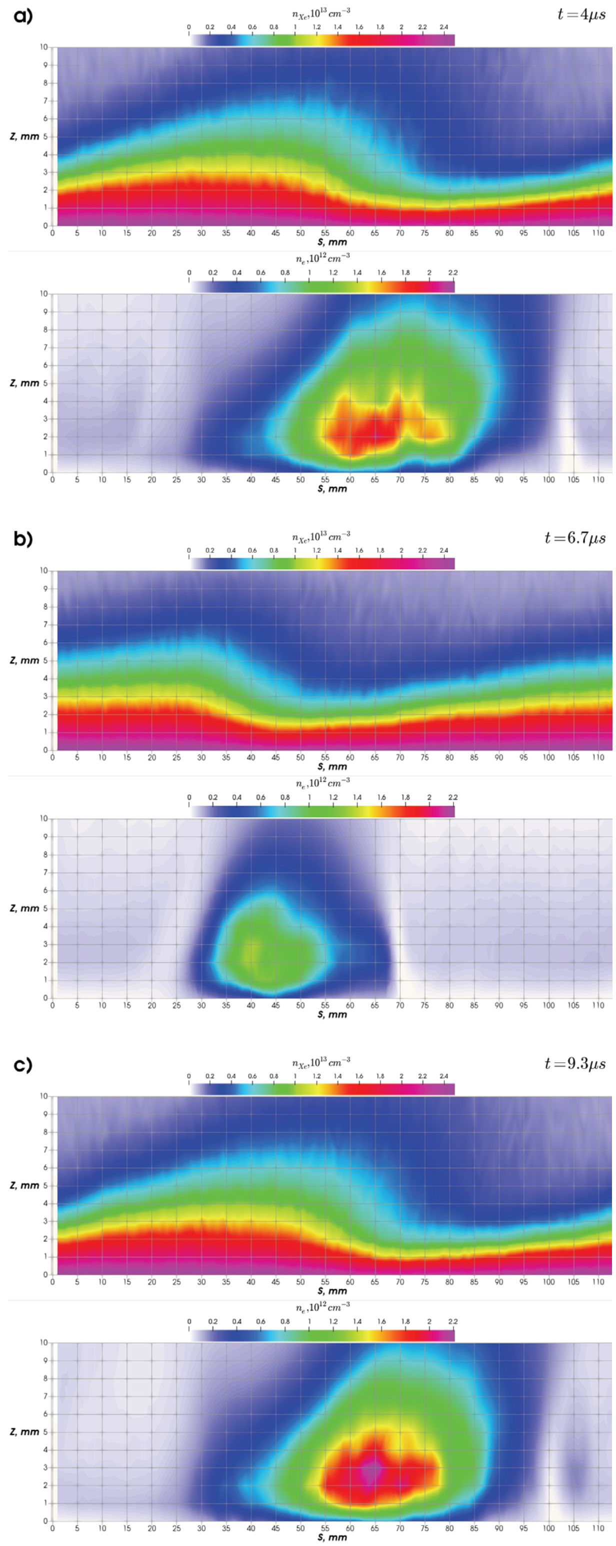

Figure 11. Evolution of the plasma and neutral density at the spoke radius $R_{Sp} = 18$ mm during one breathing mode cycle. The azimuthal distance S is measured counter-clockwise. The timestamps on the colormaps correspond to the timescale of Fig. 10.